I. Rak, V. Gliha†, L. Sidjanin‡, and B. Petrovski§*

J Integral Testing of SA Weldments on HSLA Steel with Different Treatments after Welding

REFERENCE Rak, I., Gliha, V., Sidjanin, L., and Petrovski, B., ***J* integral testing of SA weldments on HSLA steel with different treatments after welding**, *Defect Assessment in Components – Fundamentals and Applications*, ESIS/EGF9 (Edited by J. G. Blauel and K.-H. Schwalbe) 1991, Mechanical Engineering Publications, London, pp. 861–878.

ABSTRACT The research work presented in this paper treats fracture toughness of SA weldments of low carbon Q + T steel Niomol 390 having high toughness. *J* integral and CTOD measurement was performed on the base material, HAZ, and all-weld metal, which were in as-welded, stress relieved, and vibrated and stress relieved condition. Vibration before stress relief was used to improve the toughness of the coarse grained HAZ (CGHAZ) and all weld metal by anelastic effects.

During fracture toughness testing, first of all at lower temperatures, the 'pop-in' effect appeared due to a local brittle zone (LBZ). In the all-weld metal 'pop-in' appeared already at room temperature in all three mentioned conditions. Although the Charpy toughness was satisfactory, SEM analyses indicated in the microstructure a high amount of M/A constituents and large sized fracture facets on the fracture surface at the initiation point. 'Pop-in' in the HAZ occurred at much lower temperatures then 'pop-in' in the all-weld metal. This is a consequence of better sized and fewer M/A constituents and smaller sized facets. Beneficial influence of vibration used prior to stress relieving with improvement of fracture toughness in the CGHAZ and all-weld metal was found.

Introduction to fracture toughness of weldments

Low toughness of SA multi-pass weldments often occurs. Microalloyed normalised, TMT and Q + T steels have excellent toughness at low temperature in delivered condition. To avoid the decrease of toughness in CGHAZ, lower input energy by welding is allowed. On the other hand, the toughness in all-weld metal is influenced by the selection of the consumable and the welding procedure. As the fracture properties are influenced by the thickness in addition to microstructures, the evaluation of weldment properties from the standpoint 'Fitness for purpose' should be treated according to fracture mechanics principles (**1**). Taking into consideration certain recommendations, fracture toughness as fracture mechanics parameter allows one to estimate the critical planar defect dimension under certain kinds of loading. This is the starting point to prescribe the dimension of allowable size for NDE (**2**).

To realise such an approach, the fracture mechanics testing should be carried out on the whole thickness concerned and the weakest zone in the welded joint should be found by a suitable location of the fatigue crack tip.

* Faculty of Technical Sciences, University of Maribor, Yugoslavia.
† Research and Development Institute, Metalna Maribor, Yugoslavia.
‡ Faculty of Technical Sciences, University of Novi Sad, Yugoslavia.
§ Faculty of Metallurgy and Technology, University of Beograd, Yugoslavia.

Because of the high level of residual stresses and series different structures in the welded joint, fracture due to LBZ is a serious danger. From the standpoint of integrity of the joints, thermal treatments after welding are beneficial due to stress reducing around the crack tip, but they can reduce the toughness in CGHAZ. In thicker sections, reheat cracking because of local creep at the crystal boundary and matrix interfaces may occur as well **(3)**. In some cases, inelastic phenomena, such as stabilisation of dislocations and their reactions with metal misfit atoms in the solid solution, by applying vibration before thermal stress relieving, can reduce the mentioned local creep **(4)**. The above considerations were the reason for testing fracture toughness with specimens in as-welded, stress relieved, and vibrated and stress relieved condition.

Testing procedure

Steel and welding consumable properties

Investigations were performed on a newly developed low carbon steel Niomol 390 in Q + T condition. The properties of steel and consumable are listed in Tables 1 and 2. Welding consumable giving slight overmatching properties was used.

Welding of samples and preparation of specimens

The samples were submerged arc welded by applying the multipass procedure without preheating, using an inter-pass temperature of 30°C. The used input

Table 1 Niomol 390 steel properties

				Charpy toughness, −60°C	
Thickness (mm)	*YP (MPa)*	*UTS (MPa)*	*El_5 (%)*	*Normal (J)*	*Aged condition (J)*
30	432	528	25	198, 161, 149	109, 149, 126

Chemical composition
0.08 C, 0.3 Si, 1.11 Mn, 0.015 P, 0.006 S, 0.049 Nb
0.08 Sn, 0.047 Al*, 0.18 Ni, 0.012 As; Pcm = 0.150

Al* in solid solution

Table 2 Welding consumable properties for all weld metal, SAW OP40TT + EPP2Ni, Φ 4 mm

Code	*YP (MPa)*	*UTS (MPa)*	*El_5 (%)*	*Charpy toughness, −60°C (J)*
DIN 8557/1	480	590	24	40

Chemical composition of all-weld metal
0.06 C, 0.2 Si, 0.3 Mn, 1.0 Ni; Pcm = 0.123
H_D < 2 ml/100 gr, after flux drying at 400°C
Chemical composition of joint weld metal used in this research
0.075 C, 0.25 Si, 1.0 Mn, 0.87 Ni, 0.02 Nb; Pcm = 0.149

energy was approximately 15 kJ/cm. After welding, postheating up to 200°C for 2 hours was carried out. Groove prepatation and welding sequence is shown in Fig. 1(a) **(5)**. Designation of weldment conditions are as follows:

A – as-welded;
B – stress relieved, 580°C for 3 hr;
C – vibrated and then stress relieved, 580°C for 3 hr.

CT specimens were cut out from all samples and equipped with a mechanical notch positioned in the HAZ and all-weld metal as it is shown in Fig. 1(b), for measuring *J* integral and CTOD.

Fracture properties testing of welded joint

The notch location in the HAZ and all-weld metal, shown in Fig. 1(b), was selected to determine fracture toughness and transition temperature point at which the instability after slow crack growth (SCG) appears in the form of 'pop-in', i.e., when it becomes visible on the fracture surface. Therefore the testing temperature was lowered until 'pop-in'.

For all treated cases, the intention was to determine the lower band of LBZ fracture toughness, i.e., when the fracture through LBZ occurs without earlier SCG.

J integral was measured in accordance with ASTM 813-87 **(6)** and EGF Procedure P1-87D **(7)**, while the CTOD was determined according to ASTM Committee Draft E 24/88 **(8)**.

For the comparison to the HAZ and all-weld fracture properties the measured values for base material are listed in Table 3 and plotted also in Fig. 12.

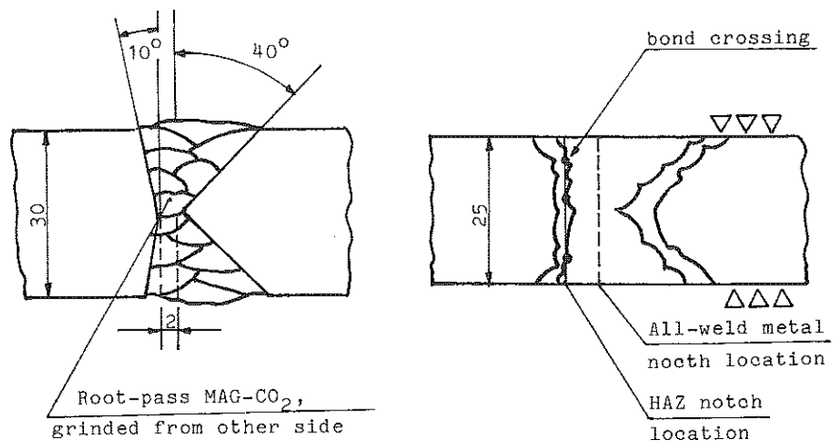

Fig 1 Shape of SAW joint and notch location

Table 3 *J* integral and CTOD values for base metal

Condition	*Designation*	*Temp.* (°C)	J_i^* (kNm^{-1})	δ_i^* (*mm*)
Base metal	P1	+20	555	0.64
	P6	+10	511	0.48
	P2	0	569	0.68
	P5	−10	597	0.68
	P3	−20	524	0.58
	P4	−30	545	0.62
	P7	−40	487	0.51

* Approximation according to **(9)**

The resistance curves J–Δa were higher than the values of J_{max} and Δa_{max} in the prescribed box according to both references **(7)(8)**, so the condition B, $a > 25J_Q/\sigma_y$ was not fulfilled to determine fracture toughness J_{IC}. Approximate estimation of fracture toughness as J_i^* and δ_i^* were achieved by reference **(9)**, which also takes into account 0.2 mm of crack extention as the initiation point. This method is suitable for very tough materials.

Determination of J *integral and CTOD in HAZ*

CT specimens with notch in HAZ were fatigue pre-cracked and loaded for J integral and CTOD measurement at different temperatures. The values are listed in Table 4(a).

The terms signify:

J_i, δ_i – value determined at start of SCG;
J_c, δ_c – value at point of 'pop-in' without earlier SCG;
J_u, δ_u – value at 'pop-in' happened after SCG;
$J_{b0.2}$, $\delta_{b0.2}$ – value at 0.2 mm crack extension before 'pop-in' **(7)**.

For the comparison Charpy toughness for condition A is added in Table 4(b).

HAZ fracture surface analyses

After loadings until occurrence of 'pop-in' effect or slow crack extension, the fracture surfaces were marked by the fatigue procedure. After final fracture surface examination the specimens were cut to check the location of fatigue crack in the thickness direction and longitudinal direction for verifying the path of SCG and LBZ location according to reference **(5)**. The HAZ fractured surfaces in all three conditions are shown in Fig. 2. SEM metallography was conducted on specimens tested at the lowest temperature.

As-welded condition – A. All fatigue crack curvatures were invalid, but in spite of that the tests were carried out normally. At the very beginning of each test loading when the J value was less than 20 kJm^{-2} a crack extension occurred at the top of a concave shaped fatigue crack front due to non-uniform loading distribution along the crack end. After this event, the normal experiment continues and the result is SCG combined with 'pop-in' or without it. This can be seen from diagram J–Δa of specimen A3 in Fig. 3(b). To prevent invalid

Table 4(a) *J* integral and CTOD values for the HAZ

Condition	*Designation*	*Temp.* (°C)	J (kNm^{-1})	$J_{b0.2}$ (kNm^{-1})	*δ-CTOD* (*mm*)	$\delta_{b0.2}$ (*mm*)
A	A4	0	$300J_i = J_{IC}$	—	$0.39 - \delta_i$	—
	A3	−10	$200J_i = J_{IC}$	—	$0.31 - \delta_i$	—
	A1	−22	$463 - J_u$	155	$0.65 - \delta_u$	0.23
	A2	−30	$413 - J_u$	150	$0.55 - \delta_u$	0.25
B	B1	−30	$285J_i = J_{IC}$	—	$0.47 - \delta_i$	—
	B2	−40	$240J_i = J_{IC}$	—	$0.35 - \delta_i$	—
	B4	−50	$30J_C$	—	$0.036 - \delta_C$	—
C	C1	−30	$300J_i = J_{IC}$	—	$0.35 - \delta_i$	—
	C4	−40	$290J_i = J_{IC}$	—	$0.25 - \delta_i$	—
	C2	−50	$340J_i = J_{IC}$	—	$0.27 - \delta_i$	—

Table 4(b) HAZ Charpy toughness for condition A in (J)

	Testing temperature (°C)						
Condition	+20	−20	−40	−50	−60	−70	−80
A	183	128	90	74	98	76	20
	184	126	84	61	77	51	14
	208	153	106	101	83	—	—

fatigue front, the procedure with two different R ratio should be used **(10)**. Partial appearance of LBZ on the fracture surface can be seen in specimen A2 of Fig. 2. The 'pop-in' event appeared at −22°C. There are two LBZs at the points where fatigue crack crossed the CGHAZ.

In the middle of the specimen, the joining of both partial LBZs occurred. Between those LBZs the fracture surface with many tough regions (cavity formation between brittle facets), caused by SCG can be recognised.

The point of initiation, which is designated by an arrow in Fig. 2, is represented in Fig. 4. A brittle fracture without any SCG can be recognised in front of the stretched zone. The mentioned effect was proved by metallographical research of specimen A2 on the cuts A–A, B–B, and C–C shown in Fig. 2. At the cut A–A the position of fatigue crack was visible. SCG at the cut B–B developed along the region of temperature AC_3/AC_1, but at the cut C–C the fractured LBZ is in the CGHAZ and the bond line.

M/A constituents in CGHAZ at the initiation point of the fractured LBZ can be seen in Fig. 5.

Stress relieved condition – B. The 'pop-in' event appeared at −50°C. Fracture surfaces of specimen B4 with three LBZ is shown in Fig. 2.

Cleavage patterns can be seen at the initiation points where fatigue crack crossed the CGHAZ.

Metallographical analyses on cut A–A showed that the bond crossing occurred three times as it is schematically shown in Fig. 1(b). Cut B–B showed

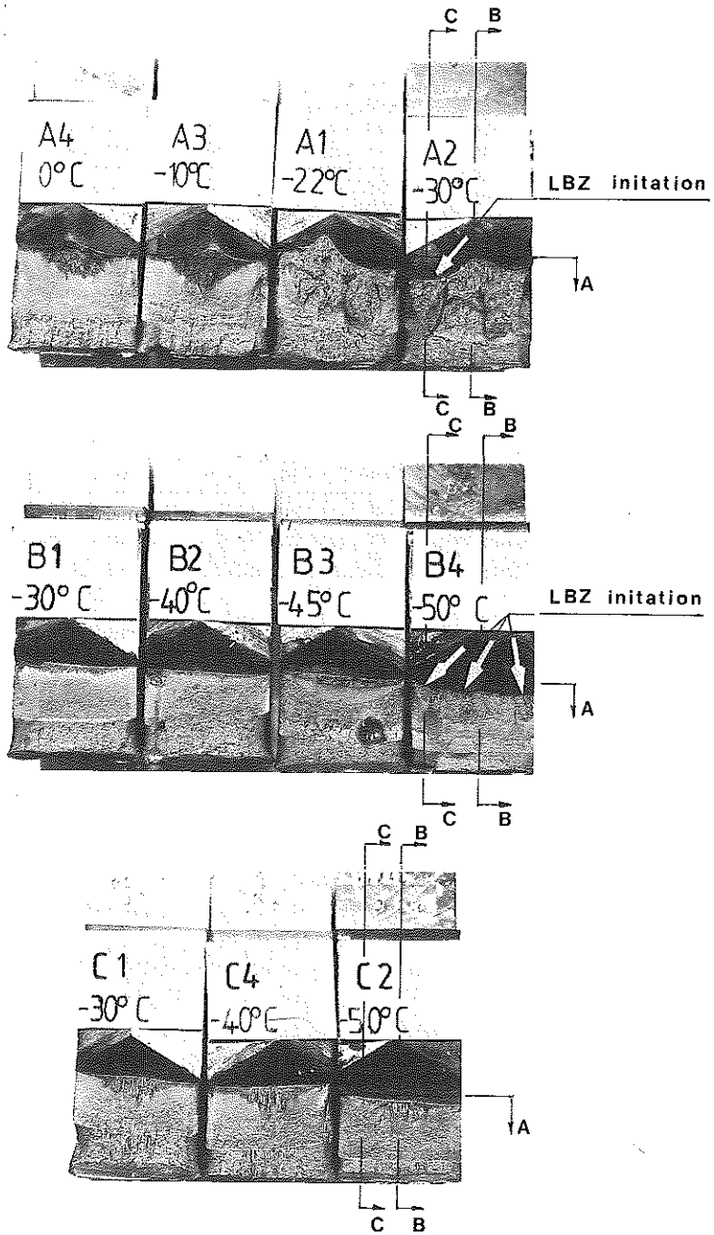

Fig 2 Fracture surfaces in the HAZ for specimens in conditions A, B, and C and cut locations

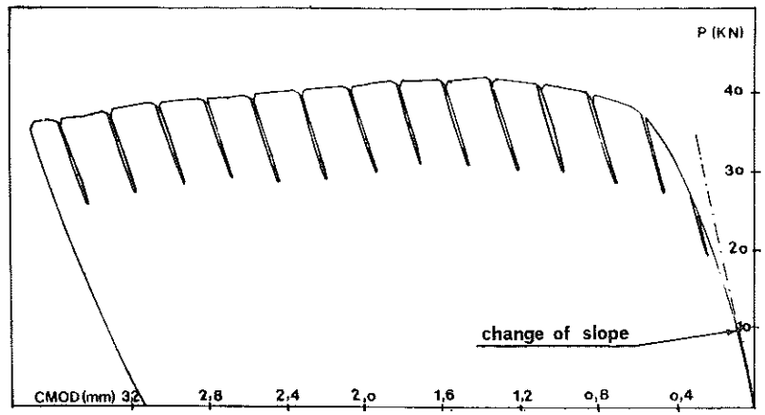

(a)

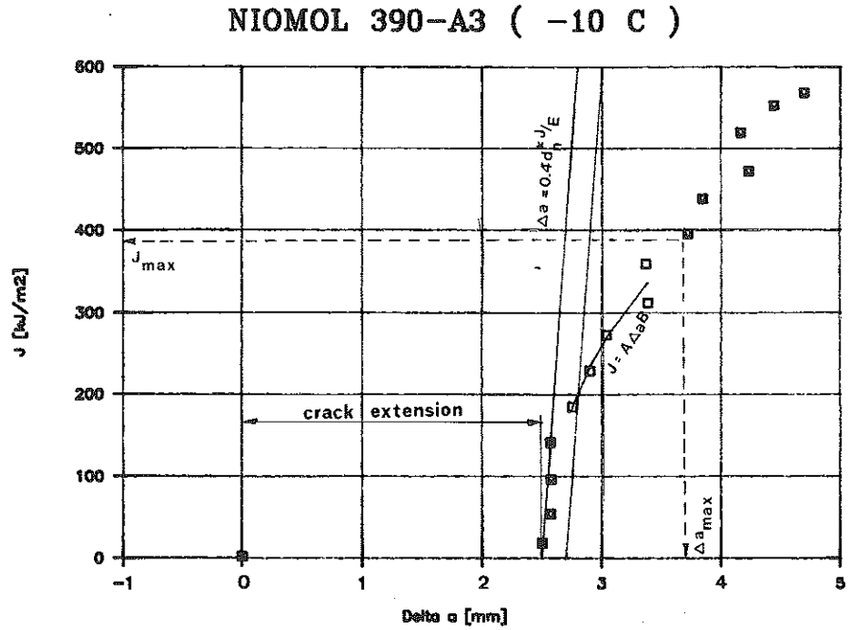

(b)

Fig 3 Crack extension at the beginning of the test in the specimen A3 at −10°C

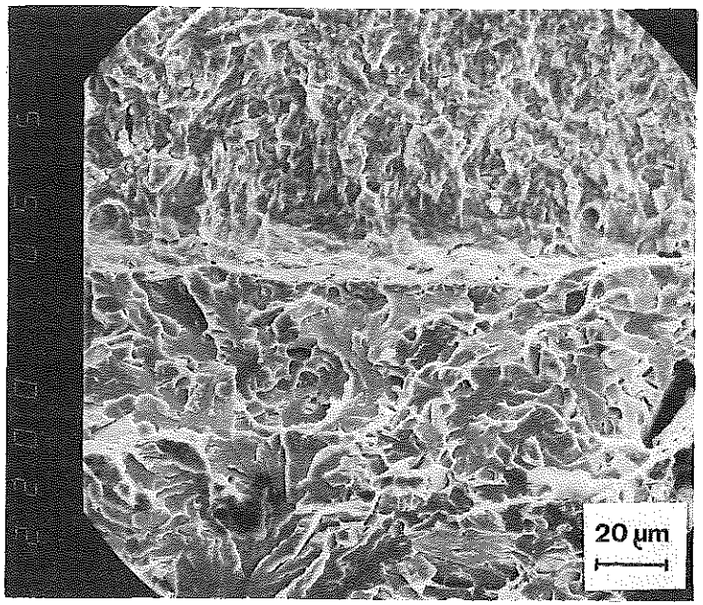

Fig 4 Fatigue crack tip blunting and transition to brittle fracture on the LBZ initiation point on specimen A2 at −30°C

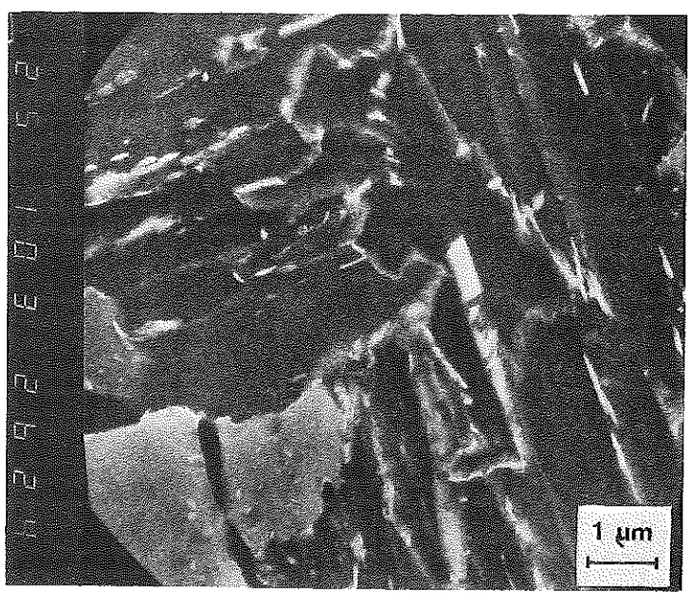

Fig 5 M/A constituents of HAZ at LBZ initiation point on specimen A2 at −30°C

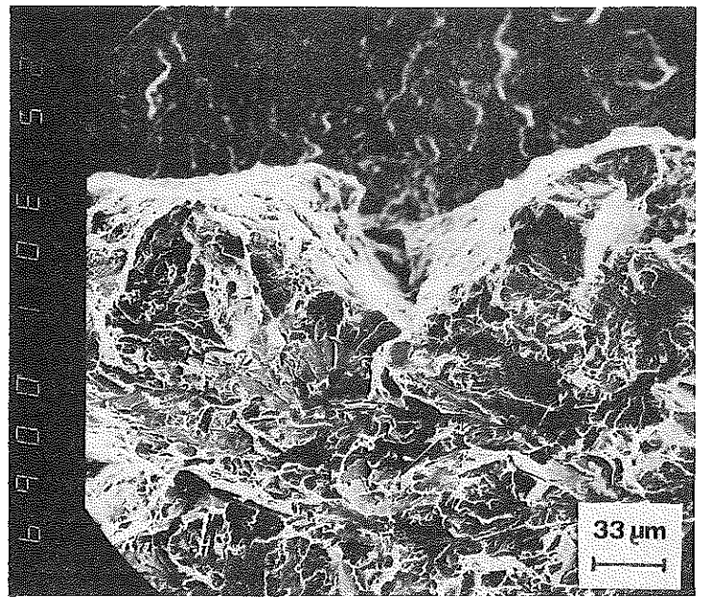

Fig 6 Transition to brittle fracture at LBZ initiation point on specimen B4 at −50°C

the AC_1 HAZ line and the fracture extension along it containing some ductile portions. Cut C–C showed also in this case cleavage fracture along CGHAZ.

The stretched zone at the fracture initiation point of LBZ on specimen B4 shown in Fig. 2 by an arrow can be seen in Fig. 6.

Vibrated + stress relieved condition – C. 'Pop-in' effect did not appear even at −50°C. Cut A–A of specimen C2 showed threefold crossing of CGHAZ by the fatigue crack. Cut B–B indicated SCG extension on the line of AC_1 HAZ, while at cut C–C the crack extension occurred along the CGHAZ as well. Figure 7 clearly indicates the stretch zone and SCG in the middle of the specimen.

Determination of J integral and CTOD in all-weld metal

Testing of fracture toughness was conducted at temperatures of +20°, 0°, and −20°C for all three conditions using the same procedure as for HAZ testing.

The results are listed in Table 5(a). The terms have the same signification as in Table 4(a). 'Pop-in' events occurred in all three conditions in spite of Charpy toughness which, according to codes, assures 'tough' weldments (Table 5(b)). Because of that, it was not possible to draw the resistance curve for fracture toughness J_{IC} determination.

All-weld metal fracture surface analyses

Fracture surfaces results of J integral and CTOD measurements are shown in Fig. 8. LBZ are marked by fatigue procedure after testing and are visible after

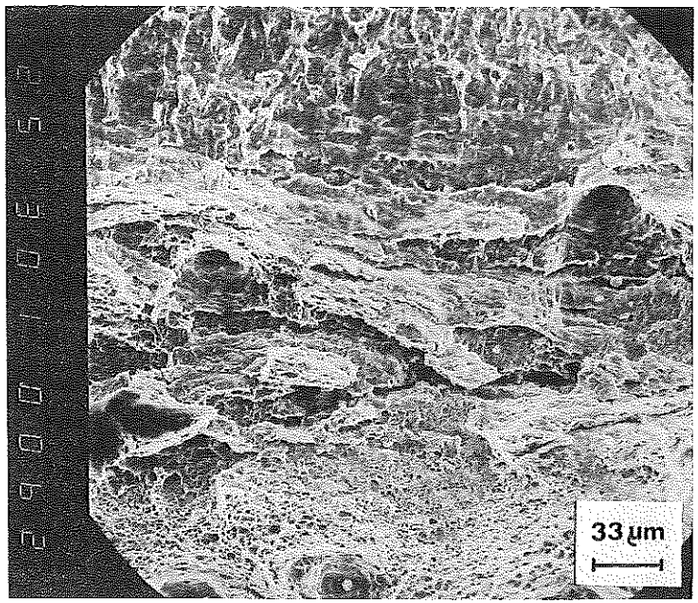

Fig 7 Stretch zone and SCG on specimen C2 at −50°C

Table 5(a) All-weld metal *J* integral and CTOD values

Condition	*Designation*	*Temp.*	J (kNm^{-1})	$J_{b0.2}$ (kNm^{-1})	*δ-CTOD* (*mm*)	$\delta_{b0.2}$ (*mm*)
A	A1	+20	$308 - J_u$	140	$0.420 - \delta_u$	0.175
	A5	0	$55 - J_c$	—	$0.062 - \delta_c$	—
	A4	−20	$72 - J_c$	—	$0.091 - \delta_c$	—
B	B1	+20	$278 - J_c$	—	$0.323 - \delta_c$	—
	B5	0	$88 - J_c$	—	$0.103 - \delta_c$	—
	B4	−20	$47 - J_c$	—	$0.062 - \delta_c$	—
C	C1	+20	$334 - J_u$	175	$0.419 - \delta_u$	0.205
	C5	0	$139 - J_c$	—	$0.153 - \delta_c$	—
	C4	−20	$83 - J_c$	—	$0.095 - \delta_c$	—

Table 5(b) All-weld metal Charpy toughness for conditions A, B, and C in (J)

	Testing temperature (°C)					
Condition	+22.5	0	−20	−40	δ_c^*, −20°C (*mm*)	$J = m\sigma_y\delta_c^*$, −20°C (kNm^{-1})
A	108	106	78	52	0.108	79
B	102	103	65	56	0.102	75
C	97	94	62	52	0.097	71

δ_c^* – CTOD determined from the reference **(11)**

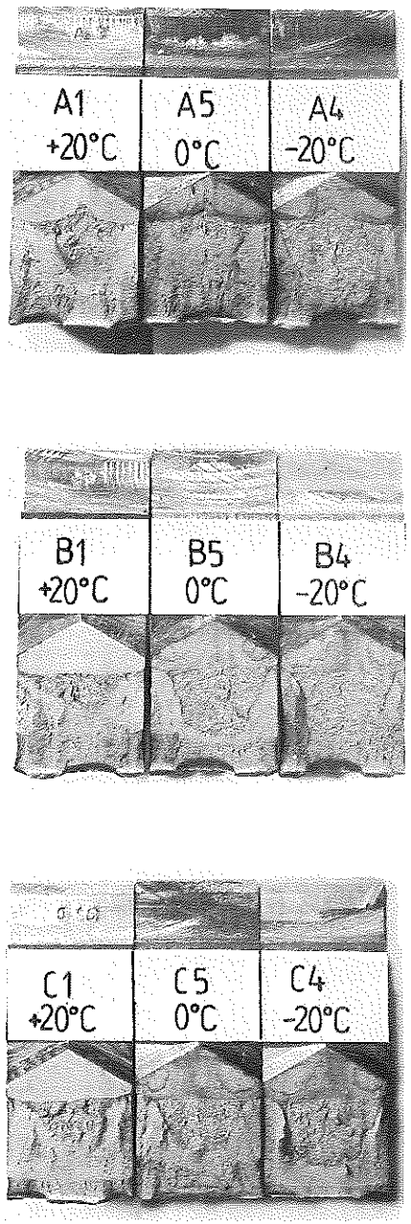

Fig 8 Fracture surfaces in all-weld metal for conditions A, B, and C

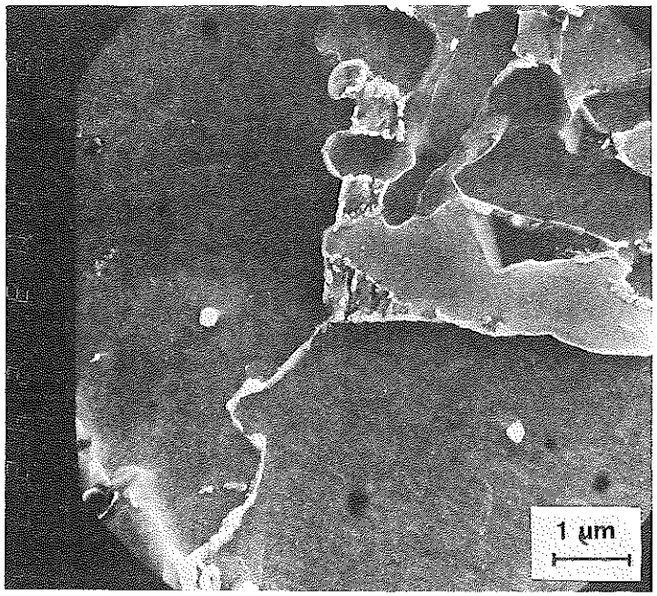

Fig 9 M/A constituents in specimen A4

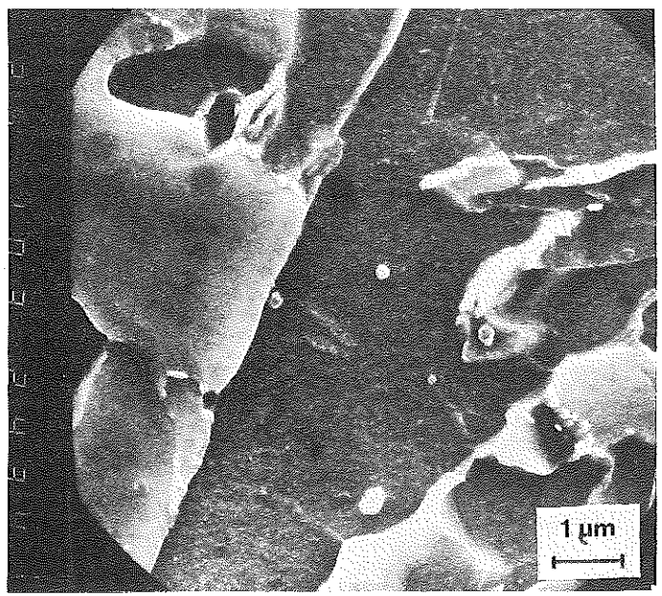

Fig 10 M/A constituents in specimen B4

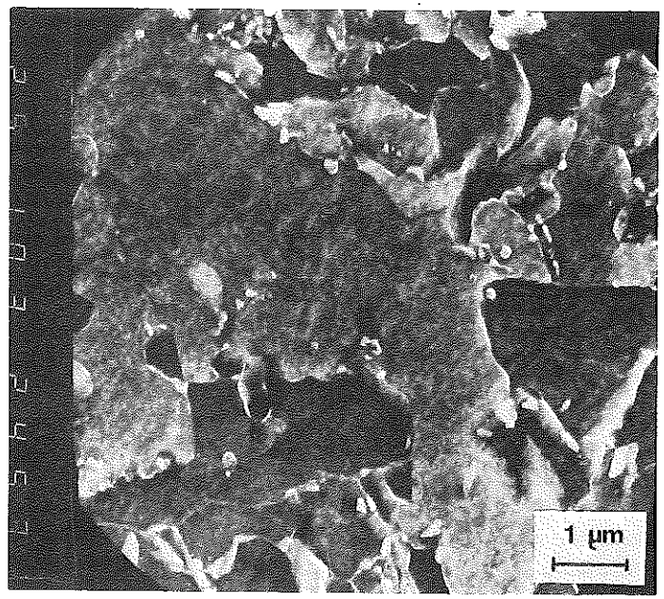

Fig 11 M/A constituents in specimen C4

final fracture of specimens. In case of specimens A1 and C1, the 'pop-in' effect appeared after SCG, while in all other cases very small Δa was followed by a momentary 'pop-in' event which was visible only on SEM. As it was seen in HAZ testing the beneficial effect of vibration on improvement of resistance properties can be noticed even more clearly because of a reliable crack position in the all-weld metal, compared to that in HAZ (Fig. 1). SEM metallography showed in the fracture surface of vibrated + stress relieved condition the greatest amount of ductile portions and the smallest region of brittle fracture immediately after the initiation point. The careful examination of the ductile portion in the fracture surface at higher magnifications showed smaller cavities but the amount of precipitated carbides and nitrides in them was higher than in other discussed condition. Special attention was paid to M/A constituent analyses in all three cases A, B, and C on specimens tested at $-20°C$. The microstructure on the fracture starting point is shown in Figs 9, 10, and 11.

Fracture toughness temperature dependence

The diagrams of J integral values versus testing temperature for all three conditions for HAZ and all-weld metal are presented in Fig. 12. The lowest measured values regardless of meaning are adopted as fracture toughness. Other measured values of J integral are also added. Values of different meaning are

connected with a dashed line. These results can be compared to the base metal toughness (BM).

Discussion

As it is shown by this paper, fracture toughness of individual microstructure parts of a multi-pass welded joint can differ a lot due to welding consumable, welding procedure, and treatment after welding in spite of the selected high toughness base metal. One can see from Tables 4(a) and 5(a) as well as from Fig. 12 that the lowest fracture toughness is measured in all-weld metal, where even at $+20°C$ the condition for J_{IC} determination was not fulfilled at all treated conditions. The more or less cleavage fracture of LBZ appeared after a short SCG or immediately after blunting of fatigue crack tip. Thermal stress relieving of all weld metal did not improve the fracture toughness at all. The temperature of 580°C for 3 hours (which is enough for relieving high residual stresses) is too low for decomposition of M/A constituents which, due to all-weld metal quenching ability, appeared in great quantity and massive shape. Only the formation of cementite can be seen at the edges of the M/A constituents/ferrite interfaces. In case of prior vibrated specimens the process of M/A constituents decomposition is more visible, because a greater quantity of cementite and occurrence of precipitation beginning of other metal carbides can be noticed.

The comparison of the above mentioned precipitation kinetics with the base metal shows the total decomposition of M/A constituents, which are fewer but massive in shape.

Non-coherent and semi-coherent precipitates can be seen in ferrite and even the coherent ones can be anticipated under the magnifying glass.

The HAZ fracture toughness values are higher than those of all-weld metal. On the Fig. 12 one can notice a better toughness of HAZ even at somewhat lower temperatures.

LBZs in HAZ are visible in as-welded condition at $-22°C$, but the corresponding value for J and CTOD do not represent their fracture toughness. The reason is SCG in tougher structure before 'pop-in' appearance. Thermal stress relieving improves the toughness, so the first LBZ was found at $-50°C$. The determined value represents the fracture toughness of the LBZ, because the 'pop-in' event occurred before SCG; this finding is in conformity with reference **(12)**. Improvement of toughness can be explained by the continuation of precipitation started in as-welded condition from less over-saturated solid solution of fewer M/A constituents present in the microstructure of HAZ. Even in this case prior vibration is beneficial. The LBZs did not fracture even at $-50°C$, so the resistant curve was drawn and J_{IC} was determined.

The LBZ fracture toughness depends considerably on the fracture facet size and on the quantity of M/A constituents **(13)**. So an attempt to use formulations which correlate both parameters with CTOD value equal 0.25 mm temperature and Charpy transition temperature was made **(14)**.

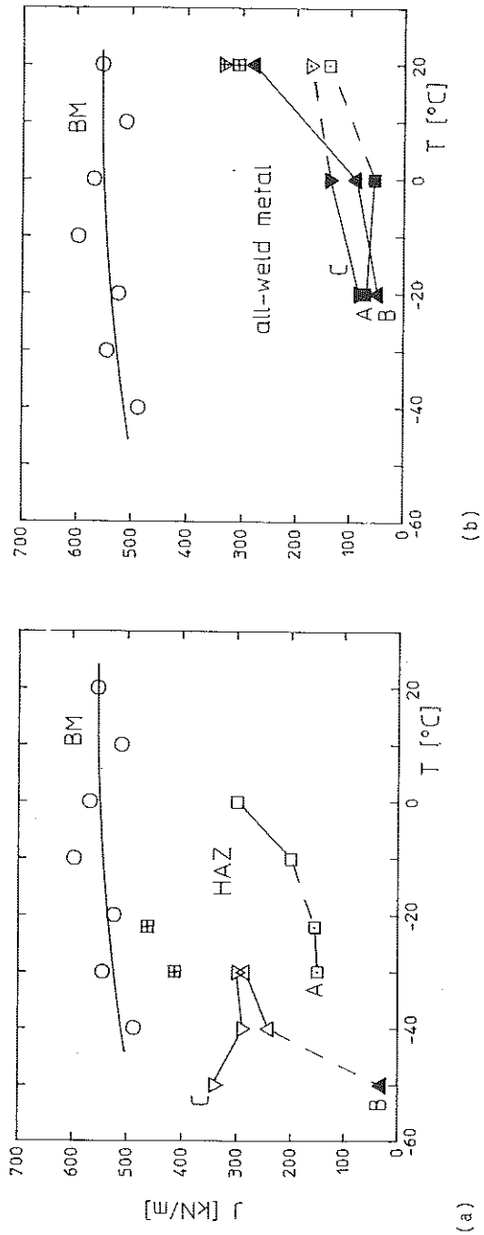

Condition	A	B	C
J_i - SCG initiation point = J_{Ic}	□	△	▷
J_c - "pop-in" without apparent SCG = cleavage fracture	■	◀	▶
J_u - "pop-in" after SCG	⊞		⊳
J_{a2} - J at 0.2 mm crack extension before "pop-in"	⊡		▷

Fig 12 ***J*** **integral of HAZ and all-weld metal versus temperature for conditions A, B, and C**

Table 6 Amount of M/A constituents and fracture facet size of LBZ, and corresponding transition temperatures

Fractured at	*d (mm)*	*M/A (%)*	*T* ($\delta_c = 0.25$) (°C)	*vTs* (°C)	*T* (80 *J*) (°C)
−20°C, all-weld metal (A4)	0.0186	11.0	+63	−19	−19
−30°C, HAZ (A2)	0.0118	8.8	+22	−46	−49

$$T(\delta = 0.25 \text{ mm}) = -10d^{-1/2} + 10.3(\text{M/A}) + 296.4 \quad (1)$$

$$vTs = -10.3d^{-1/2} + 3.4(\text{M/A}) + 291.9 \quad (2)$$

where

T, vTs are temperature and Charpy transition temperature in (K)
d is average fracture facet size in (mm)
M/A is the fraction of M/A constituents in percent

For as-welded condition for HAZ and all-weld metal the avarage fracture facet size and quantity of M/A constituents were estimated. The results are given in Table 6. Thus the structure in as-welded condition, found at the initiation point of LBZ, should have $\delta_c = 0.25$ mm at a temperature of +63°C for all-weld metal and +22°C for HAZ. Charpy transition temperature vTs should be −19°C for all-weld metal and −46°C for HAZ. These temperatures are comparable to the measured Charpy toughness values from Tables 4(b) and 5(b) if the transition temperature is defined as temperature of approximately 80 J. The comparison with measured fracture toughness values is not possible due to different temperature range. The further problem is how to determine the lowest fracture toughness off scatter band and also the problem of notch positioning in HAZ. We assume that the determination of the lowest facture toughness in the multi-pass weldment by locating the fatigue pre-crack in the weakest part of CGHAZ as near as possible to the middle of the thickness is the most suitable. This is the consequence of more pronounced plane strain in the middle of the specimen. The lowest measured value of CTOD and the highest temperature, where the 'pop-in' effect appears without SCG, should be used as LBZ fracture toughness. This complies with references **(12)** and **(15)**. In accordance with the above considerations, it is suitable to compare the values for HAZ, obtained on real weldments, with those obtained on the simulated structures. Single and multi-thermal welding simulation cycles have to be considered. In this case the uncertainties in fatigue pre-crack positioning are excluded and fracture properties of the desired region of CGHAZ and its susceptibility to contain the LBZ can be tested at all necessary temperatures.

Conclusions

From the presented introductory research work, which will be followed by extended research of different welded joint regions, we have come to the following conclusions:

In case of welding of high toughness micro-alloyed HSLA steel containing $C < 0.1$ percent, welded without preheating because of low Pcm and H_D, using lower heat input to improve HAZ toughness, M/A constituents can appear in the remaining parts of CGHAZ, which due to shape, distribution, and degree of oversaturated solution, can considerably influence the fracture toughness of HAZ.

HAZ fracture toughness can be improved by the use of thermal stress-relief and first of all of prior vibration due to beneficial precipitation processes (if the steel is not susceptible to reheat cracking), for lowering the highest hardnesses and reducing the internal micro-stresses because of dislocation stabilisation, especially at the crystal bounary/matrix interfaces, if the conditions for anelastic effects in the micro-structure are made possible. SEM examination and reference **(4)** prove that vibration accelerates the precipitation processes on the basis of anelastic effects at the stress relieving temperature.

All-weld metal has the lowest fracture toughness of whole joint, which was not much improved by thermal stress relieving. No precipitation processes in M/A constituents at the LBZ initiation point in as-welded condition were noticed. Fracture toughness in stress relieved condition was slightly improved by the prior use of vibration. In this case greater quantity of ductile regions was found in the fracture surface of the LBZ. The temperature of 580°C was obviously not high enough to cause a visible M/A constituents decomposition.

Charpy toughness values which fulfil the minimum code requirements for weldment quality estimation, are not enough for assuring of fracture properties. Even in the case of all-weld metal with Charpy toughness higher than 50 J at −40°C, LBZ at +20°C after short SCG for a specimen 25 mm thick appeared. The reason could be the exclusion of thickness constraint effect at Charpy testing. For estimating the real importance of LBZ occurrence in the welded joint, wide plate tests should be used **(16)(17)**.

Determination of the lowest value of LBZ fracture toughness by testing of welded joints is possible in case of appearance of the 'pop-in' effect, but only if the brittle initiation without SCG is following crack tip blunting.

A relationship between fracture facet size and amount of M/A constituents at the LBZ initiation point enables forecasting LBZ fracture toughness as the weakest point in the welded joint.

Susceptibility to LBZ formation is influenced by the composition of the base metal. This is why the steel producer should be contacted before the steel is used to check the possibility of welding properties guarantee and to select the proper welding consumable for the suitable welding technique for highly loaded welded steel structures.

References

(1) SATOH, K., TOYODA, M., and NINAMI, F. Thickness effect in fracture toughness of steel welds, IIW Document X-1135-87.

(2) IIW SUB-COMMISSION XE, Guidance on methods for assessing the significance of weld imperfections on service performance with respect to fracture, IIW-Document X-1178-88.
(3) RABE, W. and RUGE, J. (1976) Zum Problem der Versprödung niedriglegirter Feinkornbaustähle beim Spannungsarmglühen, *Schweissen und Schneiden*, November.
(4) RAK, I. and LEGAT, J. (1989) Vibration use prior to thermal stress relieving for improving the HAZ ductility at high temperatures in HSLA steel weldments, 2nd International Conference on Trends in Welding Research, Gatlinburg, TN.
(5) SATOH, K. and TOYODA, M. Guideline for fracture mechanics testing of WM/HAZ, IIW-Document X-1113-86.
(6) ASTM E 817-87, *Standard test method for* J_{IC}, *a measure of fracture toughness*, ASTM, Philadelphia.
(7) SCHWALBE, K.-H., NEAL, B. K., and INGHAN, T. (1988) Draft EGF recommendations for determining the fracture resistance of ductile materials EGF Procedure P1-87D, VIII, Symposium 'Verformung und Bruch', Magdeburg.
(8) ASTM COMMITTEE E 24 (1988) Draft standard test method for crack-tip opening displacement fracture toughness measurement, ASTM, Philadelphia.
(9) TAKAHASHI, H., KHAN, M. A., and SUZUKI, M. A single specimen determination of J_{IC} for different alloy steels, *J. Testing Evaluation*, **8**, 63–67.
(10) KOCAK, M., YAO, S., and SCHWALBE, K.-H. (1989) Effect of welding residual stresses on fatigue precracking of CTOD specimens, Int. Conf., Residual Stresses – 89, Los Angeles, CA.
(11) HAGIAWA, Y., SOYA, I., TANAKA, T., and TANIGUCHI, N. (1984) Fracture assessment of welded joints – wide plate tests with welding misalignments and relation to Charpy test, *Fracture Toughness of Weldments, MPC-22*, ASME, New York.
(12) KOCAK, M., SCHWALBE, K.-H., CHEN, L., and GNIRSS, G. (1988) Effects of notch position and weld metal matching on CTOD of HAZ, Weldtech, London.
(13) IKAWA, H., OSHIGE, H., and TANOE, T. Effect of martensite-austenite constituents on HAZ toughness of a high strength steel, IIW-Document IX-1156-80.
(14) KOMIZO, Y., FURUSAWA, J., and FUKADA, Y. (1989) Development of high tensile strength steel plate with high toughness in heat affected zone, JOM 4, Helsingor.
(15) McHENRY, H. I. and DENYS, R. M. (1989) Measurement of HAZ toughness in steel weldments, V. School of Fracture Mechanics, *Fract. Mech. Appl. in Lifetime Estimation of Power Plant Components*, Dubrovnik.
(16) DENYS, R. Incentives for fracture toughness testing; IIW-Document X-1136-86.
(17) DENYS, R. Tentative guidance notes for wide plate testing, IIW-Document X-1138-87.